Comparison of Systematically Functionalized Heterogeneous and Homogenous Glycopolymers as Toxin Inhibitors

Benjamin Martyn,[1] Caroline I. Biggs ,[1] Matthew I. Gibson [1,2]

[1]Department of Chemistry, University of Warwick, Gibbet Hill Road, Coventry CV4 7AL, United Kingdom
[2]Warwick Medical School, University of Warwick, Gibbet Hill Road, Coventry CV4 7AL, United Kingdom
Correspondence to: M. I. Gibson (E-mail: m.i.gibson@warwick.ac.uk)

Received 10 October 2018; Accepted 30 October 2018
DOI: 10.1002/pola.29279

ABSTRACT: Multivalent glycosylated polymers and particles display enhanced binding affinity toward lectins compared to individual glycans. The design of glycopolymers with selectivity toward pathogen-associated lectins (toxins) for sensing or in antiadhesion therapy is complicated due to lectins having promiscuous binding profiles and can be considered to be pattern recognition "readers," with the capability to bind to several different glycans. Here, heterogeneous glycopolymers bearing variable densities of two different monosaccharides are synthesized by a three-step postpolymerization modification approach, enabling systematic control over composition. It is found that heterogeneous polymers displayed increased inhibitory activity, compared to homogeneous polymers, against a RCA_{120} and the cholera toxin. This demonstrates that embracing heterogeneity in glycomaterials could result in improved performance or emergent properties. © 2018 The Authors. *Journal of Polymer Science Part A: Polymer Chemistry* published by Wiley Periodicals, Inc. J. Polym. Sci., Part A: Polym. Chem. **2018**

KEYWORDS: biomaterials; biological applications of polymers; carbohydrates; glycopolymer; infection; lectin; polymers; reversible addition fragmentation chain transfer (RAFT)

INTRODUCTION Many pathogenic bacteria secrete toxins as their primary mode of pathogenicity, including *Escherichia coli* O-157 Shiga toxins (food poisoning) and the toxin from *Vibrio cholerae* (cholera).[1–4] Plant toxins can also cause significant harm, such as ricin (from *Ricinus communis*) which has a lethal dose of ~20 μg kg^{-1} and is more toxic than cyanide.[5] A common feature is that these proteins contain a carbohydrate binding domain to hijack host cell-surface glycans and gain entry. Carbohydrate–protein interactions mediate a huge range of recognition/signaling events including inflammation,[6] immune-responses,[7] and cell–cell signaling.[8] The "reader" proteins that mediate these interactions are known as lectins, which typically have very weak binding affinities (mM).[9] Nature therefore presents multiple copies of each glycan, giving a nonlinear increase in affinity, known as the "cluster glycoside effect."[10,11] This has inspired the use of glycomaterials, such as polymers or particles, which use polyvalent presentation of carbohydrates to enhance affinity.[12,13] This enhanced affinity offers a route to prophylactic antiadhesion therapies against pathogens/toxins, as an alternative to traditional antibiotics or small molecule drugs.[14] "STARFISH" glycodendrimers have 10^6-fold enhanced activity against Shiga toxins compared to the free glycan,[15] linear poly(mannose) is a nM inhibitor of DC-Sign/GP120 interactions,[16] and inhibition of the Ebola virus by a 120-valent mannose glycofullerene cluster has been observed.[17] High affinity sialic acid glycopolymer arrays have been used by Godula and coworkers to dissect how influenza engages with its host.[18] While these multivalent systems all show high avidity, they typically present monosaccharides and hence do not have high specificity. Glycopolymers have been developed by Kiick and Polizzotti[19] and Gibson and coworkers[20,21] with high affinity for the cholera toxin by modulation of the linker length to match the binding pocket depth, increasing affinity without additional synthetic complexity. In addition to the chemical complexity of oligosaccharides, cell surfaces are heterogeneous and dynamically display many different glycans.[22] Evidence is emerging that these lower affinity glycans play a key role in the overall affinity, and that reproduction of this heterogeneity in glycomaterials can enhance avidity.[23] García Fernández and coworkers have shown that lectin binding to β-cyclodextrin-based heteroglycoclusters exhibit strong synergistic binding effects, termed the "heterocluster effect."[24] Percec and coworkers have introduced nonbinding glycans into amphiphilic Janus glycodendrimers resulting in a 12-fold increase in agglutination activity for the particles.[25] Wu and coworkers reported that cholera

Additional supporting information may be found in the online version of this article.

© 2018 The Authors. *Journal of Polymer Science Part A: Polymer Chemistry* published by Wiley Periodicals, Inc.

This is an open access article under the terms of the Creative Commons Attribution License, which permits use, distribution and reproduction in any medium, provided the original work is properly cited.

toxin has increased binding capacity toward mixtures of GM2 and fucosyl-GM1, despite homo fucosyl-GM1 having far lower binding affinity compared to homo GM2.[26] Multivalency is also observed to result in altered binding affinities compared to monovalent systems. Richards et al. have reported that mannosylated gold nanoparticles have affinity toward RCA_{120}, despite the monosaccharides having little or no affinity.[27] Sequence-controlled glycooligomers have shown increased affinity due to the nonbinding glycan providing steric shielding rather than more binding[28,29] and mixed-carbohydrate particles have been shown to have increased cell uptake into macrophages over the homogeneous equivalents.[30] This present work investigates the impact of sequentially modified heterogeneous multivalent polymer scaffolds assembled by a three-step postpolymerization methodology. It is found that addition of the second glycan has a significant effect on the overall inhibitory activity compared to homogeneous polymers and shows that screening heterogeneous polymers may enable the discovery of more active glycomaterials.

EXPERIMENTAL

2-Chloro-1,3-dimethylimidazolinium chloride, and GM1 ganglioside were purchased from Carbosynth, (Newbury, UK). D-(+)-Galactose was purchased from MP Biomedicals (Supplied by Fisher Scientific UK, Loughborough). D-(+)-mannose, triethylamine, sodium azide, pentafluorophenol, methacroyl chloride, 2-cyano-2-propyl benzodithioate, 4,4′-azobis(4-cyanovaleric acid), 1,4-dioxane, dichloromethane, dibenzocyclooctyne (DBCO)-amine, dimethylformamide (DMF), 2-aminoethan-1-ol, Greiner 384-well high-binding microliter plates, phosphate-buffered saline (PBS), HEPES, Fluorescein isothiocyanate (FITC)-labeled Ctx B, and unlabeled CTx B, were purchased from Sigma-Aldrich (Gillingham, UK). 2,6-Lutidine 99% was purchased from Acros Organics. FITC-labeled RCA_{120} and RCA_{120} were purchased from Vector Labs (Peterborough, UK). Amine reactive 2nd generation biolayer interferometry (BLI) sensors, 1-Ethyl-3-(3-dimethylaminopropyl)carbodiimide (EDC), *N*-hydroxysuccinimide (NHS), from ForteBio (Supplied by VWR, Lutterworth, UK). Ultrapure Milli-Q water was obtained from a Merk Milli-Q water purifier at 18.2 MΩ cm^{-1} resistivity at 25 °C. 3500 MWCO "SnakeSkin" dialysis tubing was purchased from Thermo Fisher (Loughborough, UK).

Physical and Analytical Methods

^{1}H, nuclear magnetic resonance (^{13}C NMR), and ^{19}F spectra were recorded on Bruker HD-300, HD-400, and AV-500 spectrometers using deuterated solvents purchased from Sigma-Aldrich. Chemical shifts are reported relative to residual nondeuterated solvent. Mass spectrometry (MS) was performed on an Agilent 6130B single Quad (electrospray ionization [ESI]). Fourier transform infrared (FTIR) spectra were acquired using a Bruker Vector 22 FTIR spectrometer with a Golden Gate diamond attenuated total reflection cell. Raman spectra were collected on a Reinshaw inVia Reflex Raman using a 442 nm HeCd laser. Liquid handling was performed by Gilson Pipette Max. 96-well plates were read using a BioTek Synergy plate reader set at 25 °C. Ultraviolet–visible (UV–vis) spectra were obtained an Agilent Cary spectrometer. BLI was performed using a ForteBio Octet 96 RED interferometer, with the indicated probes. DMF size exclusion chromatography (SEC) was performed on a varian 390-LC MDS system equipped with a PL-AS RT/MT autosampler, a PLgel 3 μm (50 × 7.5 mm) guard column, two PLgel 5 μm (300 × 7.5 mm) mixed-D columns using DMF with 5 mM NH_4BF_4 at 50 °C as eluent at a flow rate of 1.0 mL min^{-1}. The SEC system was equipped with UV/vis (set at 280 and 461 nm) and differential refractive index detectors. Narrow molecular weight poly(methyl methacrylate) standard (200–1.0 × 106 g mol^{-1}) was used for calibration using a second order polynomial fit.

Bilayer Interferometry

Amine reactive Second-Generation BLI sensors from ForteBio were presoaked for 10 min in Milli-Q water before activation with an EDC/NHS solution. After 10 min, the sensors were moved to a solution containing the lectin at 25 μg mL^{-1} in pH 5 HEPES. After 10 min, the sensors were quenched with ethanolamine, placed in HEPES buffer at the corresponding pH to baseline for 10 min, and tested against five serial dilutions of polymer solution for 30 min. The sensors were then placed into HEPES buffer for 10 min to measure dissociation. The raw data were processed using ForteBio analysis software heterogeneous ligand model. To measure the pseudo-steady-state Dissociation constant (KDs), the dissociation steps only where plotted and fit with an exponential decay in Origin to extract the end point deflection. The end points were then plotted versus both polymer and galactose concentration and fit with logistic curves to extract a midpoint value.

Competitive Binding Assays

Here, 384-well high-binding microliter plates were incubated for 16 h with 50 μL of 1 mg mL^{-1} GM1 ganglioside dissolved in PBS solution, per well. Unattached GM1 was removed by washing extensively with PBS buffer.

Due to the relatively low solubility of the polymers, polymers were dissolved in HEPES buffered saline, and any undissolved material removed by centrifugation. Exact concentrations were determined by the DBCO absorbance at 292 nm, using a calculated value for the extinction coefficient ε as 2.00 mL mg^{-1} cm^{-1}, shown in Table S1. To perform the competitive binding assays, lectin binding assays were first performed to find the optimal concentration. Serial dilutions of FITC-labeled RCA and FITC-labeled CTx in HEPES buffered saline were made and incubated in a GM1 coated 384 well plates for 30 min at 37 °C. After this time, the plates were washed extensively with buffer to remove unbound lectin and the fluorescence. The middle of the dose-dependent binding curves were chosen, which gave concentrations of 0.13 and 0.05 mg mL^{-1} for RCA and CTx, respectively.

Polymer solutions were made up as serial dilutions in HEPES from saturated stock solutions to give a volume of 180 μL in each well. Total of 120 μL FITC labeled lectin in HEPES was

added to 180 μL of each polymer solution and incubated for 30 min at 37 °C. Total of 45 μL of the polymer FITC-labeled lectin solutions was then added to the GM1 surfaces and incubated at 37 °C for 30 min. Fluorescence was then measured at excitation/emission wavelengths of 485/528 nm. All RCA experiments were carried out 18 times, CTx B experiments were carried out in triplicate. MIC_{50} values were calculated using logistic fitting in Origin.

Synthesis of Poly(pentafluorophenol methacrylate)

Pentafluorophenyl methacrylate (PFMA; 4.7 g, 18.6 mmol), 2-cyano-2-propyl benzodithioate (55.3 mg, 0.25 mmol) and 4,4′-azobis(4-cyanovaleric acid) (35.0 mg, 0.12 mmol) were dissolved in dioxane (9 mL). A sample was removed for NMR analysis. The solution was degassed with N_2 for 30 min. The reaction was then heated to 90 °C and left for 90 min. The polymerization was quenched in liquid nitrogen and precipitated three times from pentane into THF to give a pink solid, 2.3 g 50% yield. 62% Conversion by NMR. SEC (DMF): M_w = 15,250 g mol^{-1}, D = 1.7.

^{1}H NMR ($CDCl_3$) 400 MHz, ppm: 2.42 (2H, br, CH_2) 1.72 (NC-C$(CH_3)_2$-) 1.54 (3H, br, CH_3).

^{19}F NMR ($CDCl_3$) 376 MHz, ppm: −150.35 (1F, br s), −151.44 (1F, br s), −156.97 (1F, br s), −162.11 (1F, br s).

Postpolymerization Modification of Poly(pentafluorophenol methacrylate)

Poly(PFPMA) (0.260 g, 1.0 mmol by side chain) and DBCO-amine (72 mg, 0.26 mmol) were dissolved in 3 mL DMF and left at 50 °C overnight under N_2. Reaction completion was confirmed by fluorine NMR, ratio of pentafluorophenol peaks to polymeric pentafluorophenol ester peaks was 33%. Without further workup, a large excess of 2-aminoethan-1-ol (0.5 mL, 8.3 mmol) was added, and left for a further 16 h at 50 °C. Reaction completion was again confirmed by fluorine NMR observation of only pentafluorophenol peaks. The reaction was then diluted into ultrapure Milli-Q water and dialyzed for 3 days. Total of 0.10 g of white polymer was isolated. No fluorine was observed in the NMR of the final product. DOSEY was carried out to further confirm the conjugation of the DBCO unit to the polymer.

^{1}H NMR (MeOD) 500 MHz, ppm: 7.5–7.0 (br, Benzyl) 4.42 (br, cyclooctyne ring CH_2) 3.65 (br, NH-$\underline{CH_2}$-CH_2-), 3.28 (br, -NH-CH_2-$\underline{CH_2}$-), 2.5–1.5 (br, Backbone CH_2) 1.5–1.0 (br, backbone Me).

DOSEY NMR (MeOD) 500 MHz, log(m^2 s^{-1}) = −9.25, ppm: 7.5–7.0, (Benzyl) 4.42 (br, cyclooctyne ring CH_2) 3.65 (br, NH-$\underline{CH_2}$-CH_2-), 3.28 (br, -NH-CH_2-$\underline{CH_2}$-), 2.5–1.5 (br, Backbone CH_2) 1.5–1.0 (br, backbone Me).

^{13}C NMR (MeOD) 500 MHz: 179.42 (br, C=O) 141.16 (Ar), 136.93 (Ar), 132–128 (Ar), 63.02, 61.31 (NH-CH_2-CH_2-OH), 61.08 (NH-CH_2-CH_2-OH), 60.09, 59.61, 56.93, 52.49 (Cyclooctyne Ring CH2), 46.95 (NH-CH_2-CH_2-C(=O)-DBCO), 46.56 (NH-CH_2-CH_2-C(=O)-DBCO), 43.77 (Backbone CH_2), 43.14 (Backbone CH_2) 30.93 (backbone CH3).

Synthesis of Glycopolymers

Using stock solutions of 1 mg mL^{-1} sugar azide (4.87×10^{-3} mmol mL^{-1}), 2.75 mL of each of; [Gal]:[Man],100:0, 75:25, 50:50 and 25:75 (v:v) solutions were prepared. For each glycopolymer, 2.75 mL of the corresponding azido-sugar solution was added to $p(DBCO)_{15}(HEMA)_{35}$ (5 mg, 357 nmol) in a vial. The reaction was left at room temperature overnight. To remove excess sugar, the solutions were passed through a 1000 MWCO centrifugal filter and resuspended in water three times. The resulting solution was then freeze-dried. Raman of final polymers showed no presence of alkyne peak. N.B. To give a 2.5× excess of sugar azide to polymer alkyne, the number of moles of polymer was multiplied by 15 (for each alkyne unit) and 2.5 (to give an excess of sugar).

Synthesis of Azido-Monosaccharides

2-Chloro-1,3-dimethylimidazolinium chloride (2.82 g, 16.7 mmol) was added to a solution of galactose/mannose (1.00 g, 5.6 mmol), triethylamine (7.7 mL, 55 mmol), and sodium azide (3.61 g, 55.5 mmol) dissolved in ultrapure Milli-Q water (20 mL), sitting on ice. The solution was stirred for 40 min on ice before removing the solvent *in vacuo.* Ethanol (40 mL) was added to precipitate NaN_3, filtered, and the solvent removed (repeat to ensure complete removal of NaN_3). The resulting solid was then dissolved in ultrapure Milli-Q water (10 mL) and washed three times with dichloromethane. The water layer was freeze-dried to give a yellow solid. The product was then purified on a silica column using 5:1 chloroform: methanol (Rf = 0.3) to give an off-white product. Yield: 0.98 g, 86%.

1-Azido-1-Deoxy-β-D-Galactose

^{1}H NMR (MeOD) 400 MHz, ppm: 5.57 (1H, d, $J_{1\text{-}2}$ = 4.40 Hz, H1, α anomer 23.7%), 4.67 (1H, d, $J_{1\text{-}2}$ = 8.68 Hz, H1, β anomer 76.3%), 3.96 (1H, d, $J_{1\text{-}2}$ = 3.30 Hz, H5), 3.79–3.78 (1H, m, H4), 3.77–3.75 (2H, m, H6), 3.70 (1H, dd $J_{1\text{-}2}$ = 3.42, $J_{3\text{-}4}$ = 9.78 Hz, H3) 3.53 (1H, t, $J_{1\text{-}2}$ = 9.78, H2).

^{13}C NMR (MeOD) 100 MHz, ppm: 90.55 (β C1), 89.44 (α C1) 77.21 (β C4), 75.88, 75.13, 74.23, 73.06, 72.64 (β C3), 71.20 70.32 (β C2), 69.19, 68.51(β C5), 68.20, 64.20, 63.46, 61.17, 60.94 (β C6).

MS (ESI+): Observed: 228.0 Expected: 228.17 $[M + Na]^+$.

IR: 2107 cm^{-1} ($-N_3$).

1-Azido-1-Deoxy-α-D-Mannose

^{1}H NMR (MeOD) 400 MHz, ppm: 5.46 (1H,d, $J_{1\text{-}2}$ = 1.71 Hz, alpha 100%) 3.92 (1H, d, J = 10.27 Hz) 3.86 (1H, dd, $J_{1\text{-}2}$ = 1.96, $J_{3\text{-}4}$ = 3.18 Hz,H^2) 3.78, (2H, m) 3.75–3.72 (2H, m), 3.64 (1H, t, $J_{1\text{-}2}$ = 9.54 Hz).

^{13}C NMR (MeOD) 100 MHz, ppm: Major Anomer (100%): 90.57 (C1), 78.47 (C5), 70.36 (C2), 70.37 (C3), 66.60 (C4), 61.10(C6).

MS (ESI+): Observed: 228.0 Expected: 228.17 $[M + Na]^+$.

IR: 2107 cm^{-1} ($-N_3$).

Synthesis of Pentafluorophenyl Methacrylate

Pentafluorophenol (5.4 g, 29.3 mmol) and lutidine (3.5 mL, 30.0 mmol) were added to a round-bottom flask of dichloromethane (50 mL) on ice. Methacroyl chloride (3.0 mL, 31.0 mmol) was slowly added. The reaction was stirred for 3 h on ice, before leaving at room temperature overnight. The lutidine HCl precipitate was filtered and the filtrate was washed twice with water (30 mL), dried with $MgSO_4$, and the solvent removed *in vacuo*. The product was then passed through a silica column in petroleum ether 40–60 (Rf = 0.3) to give a colorless liquid, Yield 4.7 g.

^1H NMR ($CDCl_3$) 400 MHz, ppm: 6.37 (1H, s), 5.83(1H, s), 2.01 (3H, s).

^{19}F NMR ($CDCl_3$) 376 MHz, ppm: −152.89 (2F, dd, J_{1-2} = 16.35 Hz, J_{3-4} = 6.81 Hz) -158.34 (1F, td, J_{1-2} = 21.80, J_{3-4} = 9.53 Hz) -162.63 (2F, m).

^{13}C NMR ($CDCl_3$) 100 MHz, ppm: 163.04 (C4, C=O) 142.52, 140.67, 140.14, 139.14, 138.16 (C5-10, Aromatics), 133.68 (C3, Me-**C** (=CH_2)-CO)), 129.91(C2, =CH_2) 18.18 (C1, −Me).

MS (ESI +): Observed: 253.1 Expected 253.1 $[M + H]^+$.

IR: 1760 cm^{-1} (ester), 1517 cm^{-1} (unsaturated C=C), 1086 cm^{-1} (C-O), 994 cm^{-1} (C-F).

RESULTS AND DISCUSSION

To access heterogeneous glycopolymers, a three-step postpolymerization modification strategy was developed to enable the use of a single reactive precursor, which can be sequentially modified ensuring all polymers had identical chain length distributions, Fig 1.[20] PFMA was polymerized by reversible addition–fragmentation transfer polymerization to obtain master polymers (Tables 1 and 2). The observed dispersities were higher than expected due to the elution behavior of the PPFMA in SEC, but the use of a "masterbatch" means the actual dispersity is not crucial here as each

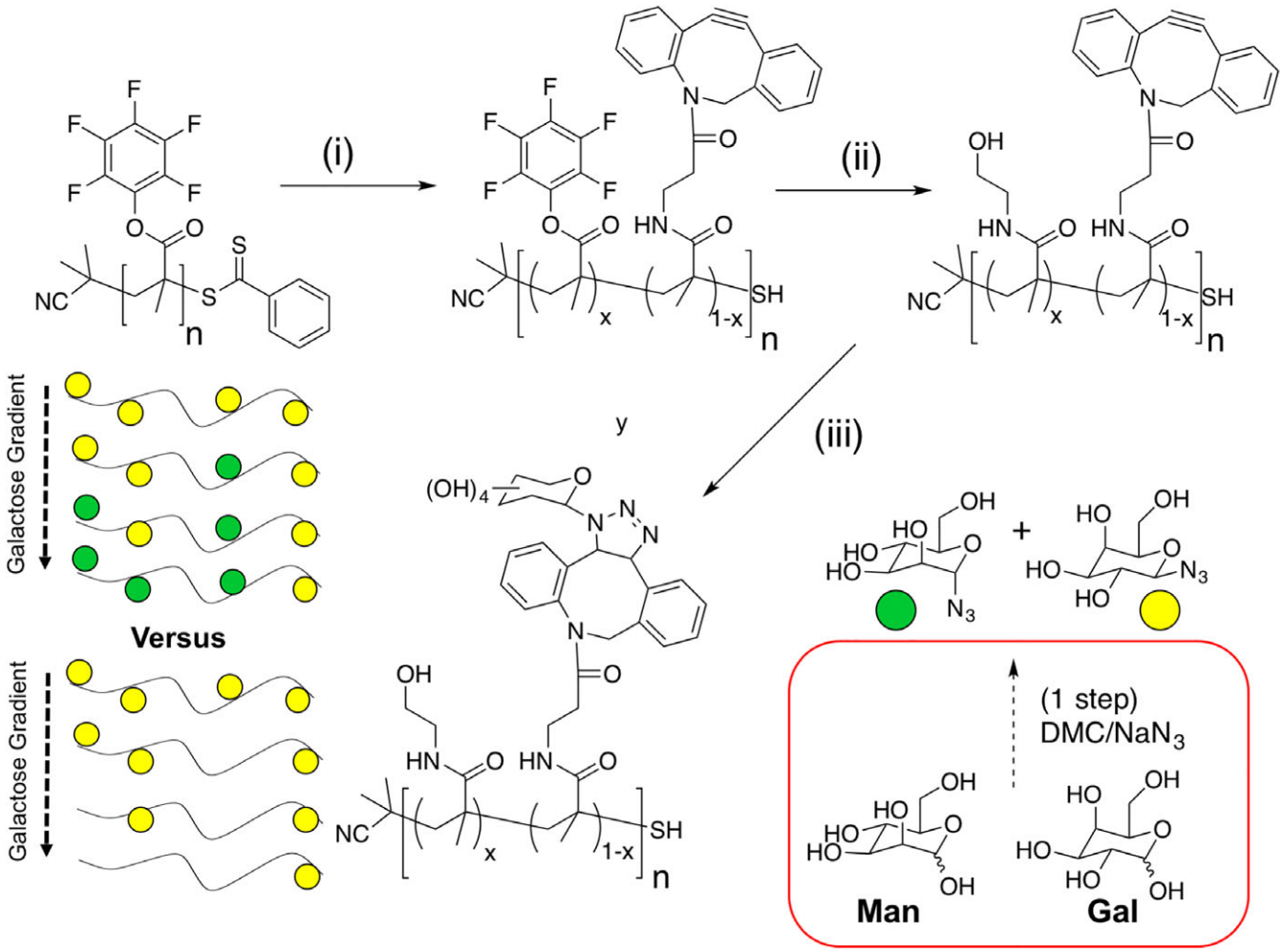

FIGURE 1 Synthesis of heterogeneous and homogenous glycopolymers. (i) DBCO (0.3 equiv/dioxane); (ii) ethanolamine (3 equiv/dioxane); and (iii) sugar-N_3 (2.5 equiv/DMF). DMC = 2-chloro-1,3-dimethylimidazolinium chloride. [Color figure can be viewed at wileyonlinelibrary.com]

TABLE 1 Heterogeneous Glycopolymers

Polymer	M_n (g mol^{-1})	M_w/M_n[a] (–)	Gal[b] (%)	Gal[c] (–)	Man[d] (–)
PPFPMA-1	8900[a]	1.7	–	–	–
$PG_{25}M_{75}$	12,900[e]	–	25	4	11
$PG_{50}M_{50}$	12,900[e]	–	50	7.5	7.5
$PG_{75}M_{25}$	12,900[e]	–	75	11	4
PG_{100}	12,900[e]	–	100	15	0

PG_xM_y refers to (galactose-functionalized polymer)$_x$ %(mannose-functionalized polymer)$_{y\%}$.
[a] From SEC in DMF.
[b] Percentage of repeat units with galactose estimated from ^{1}H NMR.
[c] Average number of galactose residues/chain.
[d] Average number of mannose residues/chain.
[e] Calculated from PPFMA precursor using conversion values.

polymer in the series will have the same distirbution.[31] ^{19}F NMR and IR spectroscopy confirmed that the PFP group was retained during polymerization (Supporting Information).

To enable introduction of the glycans by strain promoted click, DBCO-amine was incorporated into PPFMA-1 at 30 mol % followed by excess ethanolamine in a one-pot, two-stage reaction, to generate a hydrophilic, copper-free "clickable" template polymer.[32,33] Cyclooctyne incorporation was confirmed by ^{19}F NMR, IR, and Raman spectroscopy as well as ^{1}H diffusion ordered spectroscopy NMR (Supporting Information). With this reactive precursor to hand, 1-azido-1-deoxy-D-galactose ($GalN_3$) and 1-azido-1-deoxy-D-mannose ($ManN_3$) were synthesized using 2-chloro-1,3-dimethylimidazolinium chloride in a one-step procedure from the free monosaccharides.[34] It should be noted that as the DBCO unit is not symmetric, two possible regioisomers can be formed. To obtain heterogeneous, galactose-rich polymers $GalN_3$ and $ManN_3$ were mixed in the indicated ratios (Table 1) and then applied to the "clickable" precursor polymer such that the overall ratio [alkyne]:[N_3] was 1:2.5. Excess glycosyl azide was removed by dialysis and the polymers isolated by freeze-drying. For the lectin binding experiments (*vide infra*) it was necessary to have controls of homogeneous galactose-only polymers at the same overall galactose density. PPFMA-2 was modified in the same manner, but with the DBCO content varied to enable the same overall density of galactose to be introduced as in the heterogeneous library following click conjugation, Table 2.

With this panel of low density, heterogeneous/homogeneous glycopolymers to hand, their function could be tested. RCA_{120} was selected as it is a substitute for the highly toxic ricin, and our previous investigations using glycosylated gold nanoparticles revealed nonlinear behavior to galactose/mannose gradients in aggregation-based assays, suggested mannose could enhance the overall avidity/binding.[35] Fluorescently labeled lectins were incubated with each polymer, before being applied to a galactose-rich (GM1) microliter (96 well) plate.

TABLE 2 Homogenous Glycopolymers

Polymer	M_n[a] (g mol^{-1})	M_w/M_n[a] (–)	Gal[b] (%)	Gal[c] (–)
PPFMA-2	8700[a]	1.6	0	0
PG_{25}		–	25	4.9
PG_{50}		–	50	8.0
PG_{75}		–	75	10.7

[a] From SEC.
[b] Percentage of repeat units with galactose estimated from ^{1}H NMR.
[c] Total number of galactose residues/chain.

After incubation and washing the total fluorescence was measured. Less plate-associated fluorescence means more toxin inhibition. Example inhibitory curves for each set of polymers are shown in Figure 2(B,C). For the heterogeneous polymers, there is a clear dose-dependent response with increasing (polymer) leading to less lectin binding, demonstrating these are potent inhibitors of RCA_{120}. Using galactose alone, no inhibition was possible without resorting to very high concentrations, demonstrating the cluster-glycoside enhancement. Interestingly, $PGal_{100}$ (which contains no mannose) which has the highest number of expected binding units failed to fully inhibit RCA_{120} binding in the concentration range tested. In contrast, $PGal_{75}Man_{25}$ was the most active inhibitor. Polymers with intermediate Gal/Man ratios showed intermediate activity, highlighting the nonlinear effect between glycan densities and function.

Glycan density has been shown to be a key modulator of lectin affinity,[36] so to rule out galactose density leading to the above observations (rather than the mannose units), galactose homopolymers of variable density were also tested, Figure 2 (B). The homogenous polymers had similar EC_{50} values (point where activity reaches 50% of their maximum activity) to what is seen for heterogeneous counterparts. However, the total level of inhibition (i.e., how much RCA_{120} was stopped from binding) was significantly less than was observed for the heterogeneous polymers. A comparison is shown in Figure 2 (C) showing the total inhibition at the highest concentration used. This clearly demonstrates that at all galactose compositions, addition of mannose units resulted in significantly more toxin inhibition, with the heterogeneous polymers appearing to "capture" more toxin. The homopolymers all gave <50% maximal inhibition, demonstrating them to be rather poor inhibitors. These results may suggest affinity or a secondary binding site for RCA_{120} and Man which could lead to this enhancement, and explain why the IC_{50} of the polymers were similar in terms of galactose density. It is important to note that these glycopolymers had relatively poor solubility (see

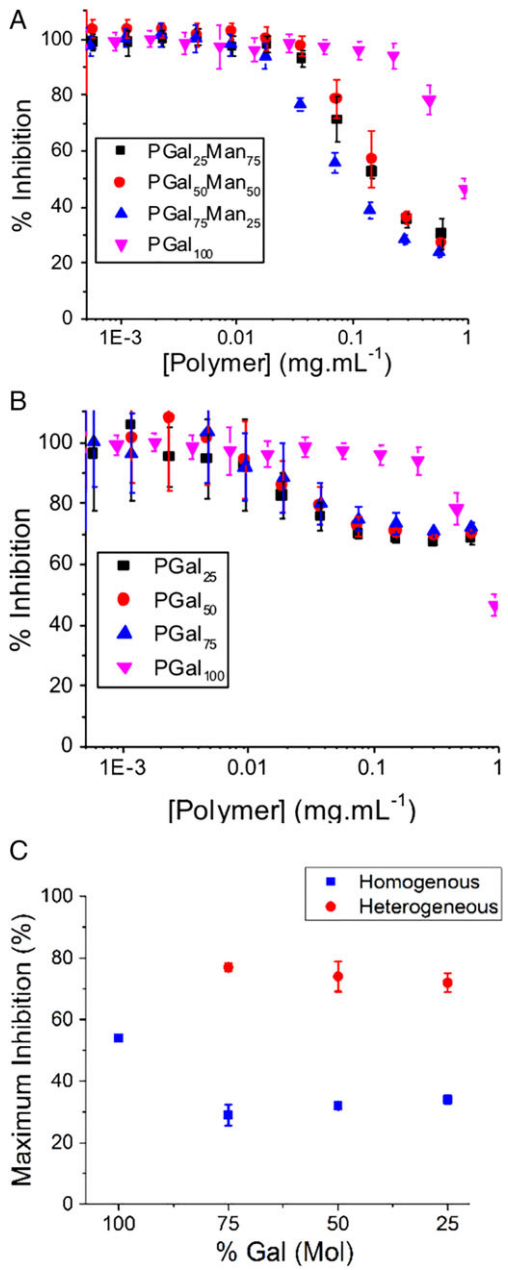

FIGURE 2 Competitive inhibition of glycopolymers against RCA_{120}. (A) Inhibition curves for heterogeneous glycopolymers; (B) inhibition curves for homogeneous glycopolymers; and (C) comparison of total maximum inhibition achieved. Inhibitory experiments were average from 18 repeats and error bars are ±SD. [Color figure can be viewed at wileyonlinelibrary.com]

Supporting Information), but there was no evidence of aggregation or self-assembly, which would impact the binding data.

The increased inhibitory activity upon including mannose might seem counterintuitive as mannose is not a strong binder of RCA_{120} on its own. However, in nature, native glycan ligands are often branched carbohydrates enabling presentation of multiple monosaccharides which undergo separate (or allosteric) interactions[26] or the glycans also act as structure directing units to simply ensure the binding units are being presented in the correct three-dimensional location.[37] To probe the binding process in detail BLI was employed; a method related to surface plasmon resonance enabling label-free protein binding to be evaluated.[38]

RCA_{120} was immobilized onto BLI sensors by NHS coupling and the polymer library was probed for binding as a function of concentration [Fig. 3(A)]. Figure 3(B) shows an example BLI binding curve for $PGal_{25}Man_{75}$ showing the characteristic association and dissociation phases and a clear dose-dependent increase in binding. Estimating the affinity (dissociation constant, K_d) of multivalent systems is challenging due to there being a suite of individual interactions in any binding curve. Therefore, a steady-state approximation was used which is widely employed to enable comparisons to be made between systems.[39,40] The extracted K_d values are shown in terms of both galactose concentration [Fig. 3(C)] and polymer concentration [Fig. 3(D)] enabling separation of the contributing factors.

On a per-polymer basis, reducing the galactose content lead to lower K_d (higher affinity) with a sixfold difference between 100 and 25% galactose. This result is interesting as the most active polymers only had four to five galactose residues per chain, showing only a minimum number are required for significant cluster glycoside enhancements (while acknowledging these are not the most active inhibitors, as the aim is to probe heterogeneity effects). Analyzing the above data on a per-galactose basis shows the increase in affinity per galactose unit is twofold between 100 and 25% density. It was observed that $PGal_{75}Man_{25}$ (which has 11 galactose $chain^{-1}$) had the highest affinity per sugar, with significant enhancements over the homogenous system. This is in line with the inhibitory data showing that 75% galactose was the most potent in terms of EC_{50} and total inhibition achieved. This rational for optimal binding agrees with previous reports that ~30% mannose is optimal for glyconanoparticles agglutinating RCA_{120}.[27,35] These observations could support an additional binding mode for mannose, and that binding is not only due to the galactose ligands. In understanding these results, chain flexibility differences seem to be unlikely to contribute heterogeneous polymers have the same number and distribution of glycan side chains at all galactose densities due to the postpolymerization strategy used, but the aromatic linker with either β or α linkage could lead to stacking. By limiting the degrees of freedom available to the glycan with the rigid linker, we may be reducing the entropic penalty required for binding overall. The overall affinities in this system (~100 mM) are relatively weak for a glycopolymer, with nanomolar affinities often reported.[16] Spain and Cameron have shown (by Surface plasmon resonance (SPR)) that increasing valency of homogalactose polymers leads to increased affinity to RCA_{120} which at first seems in contradiction to what is seen here, but the lower density and linker effects make comparisons difficult.[39]

As a final test, the heterogeneous polymers were also evaluated for binding to CTxB (Cholera toxin B subunit) using BLI

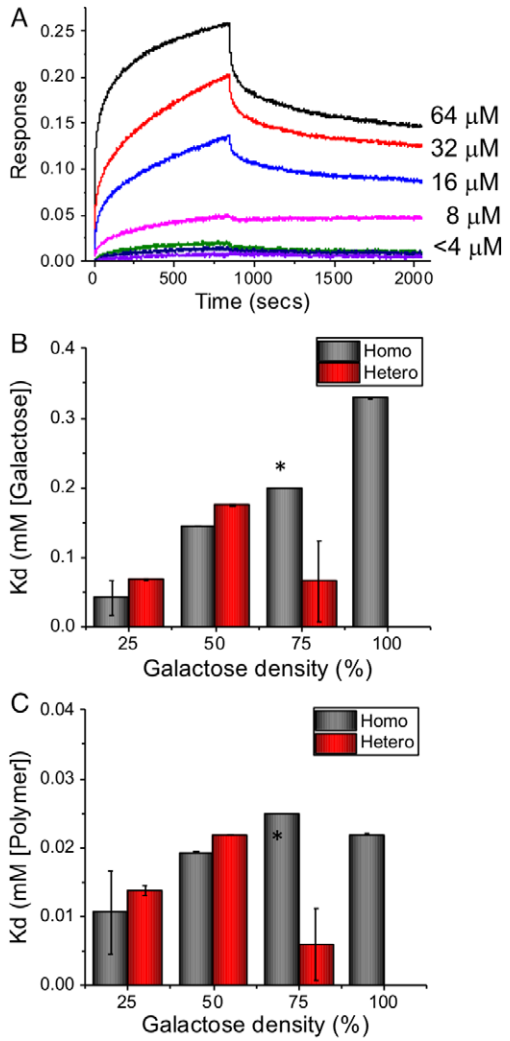

FIGURE 3 BLI analysis of glycopolymers binding to RCA_{120}. (A) Example BLI curves for serial dilution (4–64 μM) of $PGal_{25}Man_{75}$; (B) KD from 1:1 binding approximation in terms galactose concentration; and (C) polymer concentration. *Fitting parameter did not enable error to be extracted. [Color figure can be viewed at wileyonlinelibrary.com]

(Supporting Information). In line with the RCA_{120} results, heterogeneous glycopolymers resulted in increased affinity on a per polymer and per galactose basis. Due to the very high affinity of CTx for the GM1 surfaces complementary inhibitor experiments showed limited activity (Supporting Information), which may support that heterogeneity effects dominate in the lower affinity range, which has been probed in both lectins used here.

CONCLUSIONS

In conclusion, a series of heterogeneous glycopolymers with varying ratios of galactose:mannose were synthesized using a three-step postpolymerization modification strategy enabling heterogeneity effects to be separated from density effects. It was found that the inhibitory potency of the polymers against RCA_{120} (and to cholera toxin) was enhanced by addition of second glycan with a 3:1 ratio of galactose to mannose having the highest activity. BLI studies enabled estimation of the overall affinity, and in all cases lower galactose lead to lower dissociation constants (higher affinity) even though the overall affinity was rather low for a multivalent system, potentially due to the sterically large linker. Similar results were seen for another galactose binding lectin, the cholera toxin B subunit. This shows that total inhibitory activity can be modulated by using increasingly complex heterogeneous glycopolymers and that mixing distinct glycans together could give rise to unique binding modes to identify more active multivalent ligands, especially in the context of high-throughput screening.

ACKNOWLEDGMENTS

M. I. Gibson acknowledges the ERC for a Starting Grant, CRYO-MAT 638661. B. Martyn thanks EPSRC (EP/M506679/1) and UoW for a studentship and the polymer characterization Research Technology Platform (RTP) for polymer analysis.

DATA ACCESS STATEMENT

The research data supporting this publication can be accessed at http://wrap.warwick.ac.uk.

REFERENCES AND NOTES

1 T. R. Branson, W. B. Turnbull, *Chem. Soc. Rev.* **2013**, *42*, 4613.

2 G. E. Soto, S. J. Hultgren, *J. Bacteriol.* **1999**, *181*, 1059.

3 J. D. Esko, N. Sharon, *Microbial Lectins: Hemagglutinins, Adhesins, and Toxins*; Cold Spring Harbor Laboratory Press: Cold Spring Harbor, **2009**.

4 C. M. Thorpe, *Clin. Infect. Dis.* **2004**, *38*, 1298.

5 C. D. Hébert, *Toxic. Rep. Ser.* **1993**, *37*, 1.

6 L. A. Lasky, *Annu. Rev. Biochem.* **1995**, *64*, 113.

7 P. M. Rudd, T. Elliott, P. Cresswell, I. A. Wilson, R. A. Dwek, *Science* **2001**, *291*, 2370.

8 R. O. Hynes, *Cell* **1992**, *69*, 11.

9 M. Ambrosi, N. R. Cameron, B. G. Davis, *Org. Biomol. Chem.* **2005**, *3*, 1593.

10 T. K. Dam, C. F. Brewer, *Biochemistry* **2008**, *47*, 8470.

11 J. J. Lundquist, E. J. Toone, *Chem. Rev.* **2002**, *102*, 555.

12 A. Bernardi, J. Jiménez-Barbero, A. Casnati, C. De Castro, T. Darbre, F. Fieschi, J. Finne, H. Funken, K.-E. Jaeger, M. Lahmann, T. K. Lindhorst, M. Marradi, P. Messner, A. Molinaro, P. V. Murphy, C. Nativi, S. Oscarson, S. Penadés, F. Peri, R. J. Pieters, O. Renaudet, J.-L. Reymond, B. Richichi, J. Rojo, F. Sansone, C. Schäffer, W. B. Turnbull, T. Velasco-Torrijos, S. Vidal, S. Vincent, T. Wennekes, H. Zuilhof, A. Imberty, *Chem. Soc. Rev.* **2013**, *42*, 4709.

13 S. Won, S.-J. Richards, M. Walker, M. I. Gibson, *Nanoscale Horiz.* **2017**, *3*, 1593.

14 N. Sharon, *Biochim. Biophys. Acta-Gen. Subj.* **1760**, *2006*, 527.

15 P. I. Kitov, J. M. Sadowska, G. Mulvey, G. D. Armstrong, H. Ling, N. S. Pannu, R. J. Read, D. R. Bundle, *Nature* **2000**, *403*, 669.

16 C. R. Becer, M. I. Gibson, J. Geng, R. Ilyas, R. Wallis, D. A. Mitchell, D. M. Haddleton, *J. Am. Chem. Soc.* **2010**, *132*, 15130.

17 A. Muñoz, D. Sigwalt, B. M. Illescas, J. Luczkowiak, L. Rodríguez-Pérez, I. Nierengarten, M. Holler, J.-S. Remy, K. Buffet, S. P. Vincent, J. Rojo, R. Delgado, J.-F. Nierengarten, N. Martín, *Nat. Chem.* **2015**, *8*, 50.

18 M. L. Huang, M. Cohen, C. J. Fisher, R. T. Schooley, P. Gagneux, K. Godula, *Chem. Commun.* **2015**, *51*, 5326.

19 B. D. Polizzotti, K. L. Kiick, *Biomacromolecules* **2006**, *7*, 483.

20 S.-J. Richards, M. W. Jones, M. Hunaban, D. M. Haddleton, M. I. Gibson, *Angew. Chem. Int. Ed.* **2012**, *51*, 7812.

21 M. W. Jones, L. Otten, S.-J. Richards, R. Lowery, D. J. Phillips, D. M. Haddleton, M. I. Gibson, *Chem. Sci.* **2014**, *5*, 1611.

22 K. W. Moremen, M. Tiemeyer, A. V. Nairn, *Nat. Rev. Mol. Cell Biol.* **2012**, *13*, 448.

23 M. Ortega-Muñoz, F. Perez-Balderas, J. Morales-Sanfrutos, F. Hernandez-Mateo, J. Isac-Garcia, F. Santoyo-Gonzalez, *Eur. J. Org. Chem.* **2009**, *2009*, 2454.

24 M. Gómez-García, J. M. Benito, D. Rodríguez-Lucena, J. X. Yu, K. Chmurski, C. Ortiz Mellet, R. Gutiérrez Gallego, A. Maestre, J. Defaye, J. M. García Fernández, *J. Am. Chem. Soc.* **2005**, *127*, 7970.

25 S. Zhang, Q. Xiao, S. E. Sherman, A. Muncan, A. D. M. Ramos Vicente, Z. Wang, D. A. Hammer, D. Williams, Y. Chen, D. J. Pochan, S. Vértesy, S. André, M. L. Klein, H. J. Gabius, V. Percec, *J. Am. Chem. Soc.* **2015**, *137*, 13334.

26 N. C. Worstell, P. Krishnan, J. D. Weatherston, H. J. Wu, *PLoS One* **2016**, *11*, e0153265.

27 S.-J. Richards, L. Otten, M. I. Gibson, *J. Mater. Chem. B* **2016**, *4*, 3046.

28 W. G. Kreyling, A. M. Abdelmonem, Z. Ali, F. Alves, M. Geiser, N. Haberl, R. Hartmann, S. Hirn, D. J. de Aberasturi, K. Kantner, G. Khadem-Saba, J.-M. Montenegro, J. Rejman, T. Rojo, I. R. de Larramendi, R. Ufartes, A. Wenk, W. J. Parak, *Nat. Nanotechnol.* **2015**, *10*, 619.

29 D. Ponader, P. Maffre, J. Aretz, D. Pussak, N. M. Ninnemann, S. Schmidt, P. H. Seeberger, C. Rademacher, G. U. Nienhaus, L. Hartmann, *J. Am. Chem. Soc.* **2014**, *136*, 2008.

30 L. Wu, Y. Zhang, Z. Li, G. Yang, Z. Kochovski, G. Chen, M. Jiang, *J. Am. Chem. Soc.* **2017**, *139*, 14684.

31 M. I. Gibson, E. Fröhlich, H.-A. Klok, *J. Polym Sci. Part A: Polym. Chem.* **2009**, *47*, 4332.

32 N. J. Agard, J. A. Prescher, C. R. Bertozzi, *J. Am. Chem. Soc.* **2004**, *126*, 15046.

33 S. Agar, E. Baysak, G. Hizal, U. Tunca, H. Durmaz, *J. Polym. Sci. Part A: Polym. Chem.* **2018**, *56*, 1181.

34 N. Vinson, Y. Gou, C. R. Becer, D. M. Haddleton, M. I. Gibson, *Polym. Chem.* **2011**, *2*, 107.

35 L. Otten, D. Vlachou, S.-J. Richards, M. I. Gibson, *Analyst* **2016**, *141*, 4305.

36 K. Godula, C. R. Bertozzi, *J. Am. Chem. Soc.* **2012**, *134*, 15732.

37 Z. Wang, Z. S. Chinoy, S. G. Ambre, W. Peng, R. McBride, R. P. de Vries, J. Glushka, J. C. Paulson, G.-J. Boons, *Science* **2013**, *341*, 379.

38 G. Volkers, L. J. Worrall, D. H. Kwan, C.-C. Yu, L. Baumann, E. Lameignere, G. A. Wasney, N. E. Scott, W. W. Wakarchuk, L. J. Foster, S. G. Withers, N. C. J. Strynadka, *Nat. Struct. Mol. Biol.* **2015**, *22*, 627.

39 S. G. Spain, N. R. Cameron, *Polym. Chem.* **2011**, *2*, 1552.

40 S.-G. Lee, J. M. Brown, C. J. Rogers, J. B. Matson, C. Krishnamurthy, M. Rawat, L. C. Hsieh-Wilson, *Chem. Sci.* **2010**, *1*, 322.